Structural Engineering and Mechanics, Vol. 10, No. 4 (2000) 371-392
DOI: http://dx.doi.org/10.12989/sem.2000.10.4.371

Pseudo plastic zone analysis of steel frame structures comprising non-compact sections

P. Avery† and M. Mahendran‡

Physical Infrastructure Centre, School of Civil Engineering, Queensland University of Technology, Brisbane, QLD 4000, Australia

Abstract. Application of "advanced analysis" methods suitable for non-linear analysis and design of steel frame structures permits direct and accurate determination of ultimate system strengths, without resort to simplified elastic methods of analysis and semi-empirical specification equations. However, the application of advanced analysis methods has previously been restricted to steel frames comprising only compact sections that are not influenced by the effects of local buckling. A concentrated plasticity method suitable for practical advanced analysis of steel frame structures comprising non-compact sections is presented in this paper. The pseudo plastic zone method implicitly accounts for the effects of gradual cross-sectional yielding, longitudinal spread of plasticity, initial geometric imperfections, residual stresses, and local buckling. The accuracy and precision of the method for the analysis of steel frames comprising non-compact sections is established by comparison with a comprehensive range of analytical benchmark frame solutions. The pseudo plastic zone method is shown to be more accurate and precise than the conventional individual member design methods based on elastic analysis and specification equations.

Key words: pseudo plastic analysis; steel frame structures; advanced analysis; local buckling.

1. Introduction

The objective of the research described in this paper was to develop a simpler method of analysis that adequately captures the non-linear behaviour of steel frame structures comprising non-compact sections subject to local buckling effects. This simplified method of analysis must therefore be able to adequately represent the effects of local buckling in addition to the other significant factors such as material yielding, second-order instability, residual stresses, and geometric imperfections. All factors relevant to compact sections *not* subject to local buckling have been investigated by a number of other researchers who have developed concentrated plasticity advanced analysis formulations for steel frame structures comprising only compact sections. One of the most significant such formulations is the refined plastic hinge method (Liew 1992, Liew *et al.* 1993). Recently, Avery and Mahendran (1998a) have modified this formulation to suit the advanced analysis of steel frames comprising non-compact sections subject to local buckling effects. In this formulation, the effects of local buckling such as the reduction in section capacity, gradual stiffness reduction, and hinge softening are implicitly accounted for by the application of simple equations. Avery and Mahendran (1998a) demonstrated that the refined plastic hinge method is a reasonably

† Research Fellow
‡ Associate Professor

accurate technique for the advanced analysis of steel frame structures comprising non-compact sections, and significantly superior to the conventional design procedure based on elastic analysis. However, comparison with benchmark solutions identified a number of limitations and sources of error in the refined plastic hinge model, due to:

1. Simplifying approximations (e.g., initial yield, imperfections, softening, flexural stiffness reduction function, tangent modulus, and elastic stability functions).
2. The use of model parameters based on empirical specifications equations (e.g., tangent modulus, section capacity, plastic strength, and effective section properties).

Therefore a rational and more accurate method, referred to as *pseudo plastic zone* analysis, was developed to eliminate the above limitations and sources of error as a further enhancement of the refined plastic hinge method. Analytically "exact" model parameters such as the tangent modulus and section capacity were derived from distributed plasticity finite element analyses of a stub beam-column model. They were then used in the formulation of a frame element force-displacement relationship. This paper presents the details of the new method for advanced analysis of steel frame structures comprising non-compact I-sections. The new method is verified by comparison with the analytical benchmark solutions provided by Avery and Mahendran (1998b).

2. Stub beam-column model analysis

Distributed plasticity analysis can be used to calibrate accurate section capacity and stiffness reduction functions for use in concentrated plasticity models. This approach was adopted for the hardening plastic hinge method (King and Chen 1994) and the quasi plastic hinge method (Attalla *et al.* 1994) in the analyses of a typical compact section. In this paper the distributed plasticity shell finite element method of analysis described by Avery and Mahendran (1998c) was used to obtain section capacity and stiffness reduction functions suitable for non-compact sections subject to local buckling effects. Due to symmetry of the local buckling waveform, a stub beam-column model with length equal to one quarter of a local buckling wavelength could be used to obtain the required properties for a non-compact I-section. Details of the stub beam-column model are described in Section 2.1. The analytical results are presented in Section 2.2.

2.1. Description of the stub beam-column model

The stub beam-column model was developed using the same methodology as the frame models described by Avery and Mahendran (1998c). Shell elements were used in order to provide sufficient degrees of freedom to explicitly model local buckling deformations and spread of plasticity effects. The Abaqus S4R5 element was selected for all analyses (HKS 1997). This element is a thin, shear flexible, isoparametric, quadrilateral shell with four nodes and five degrees of freedom, utilizing reduced integration and bilinear interpolation schemes. A fine element mesh discretization was used (see Fig. 1) to accurately model the local buckling deformations and associated spread of plasticity. The RIKS line-arc solution method was used to obtain the softening curve. The Abaqus classical metal plasticity model with perfectly elastic-plastic behaviour (i.e., no strain hardening) was used for all analyses. This model implements the von Mises yield surface to define isotropic yielding, associated plastic flow theory, and perfect plasticity behaviour.

Local imperfections were included by modifying the nodal coordinates using a field created by

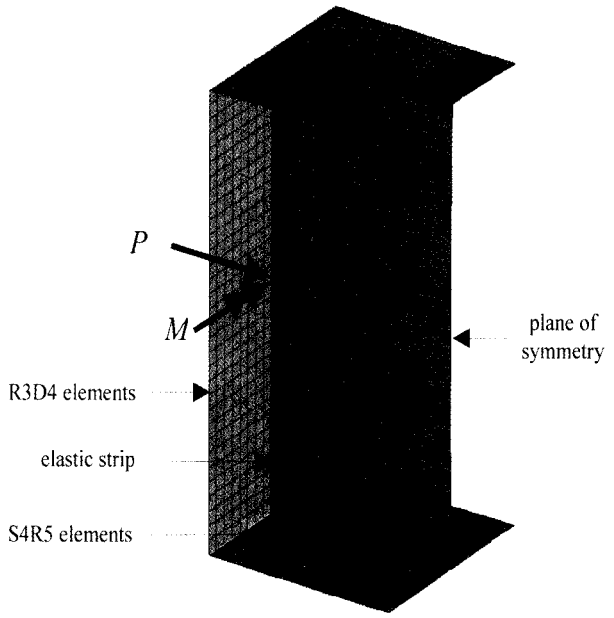

Fig. 1 Stub beam-column model geometry and finite element mesh

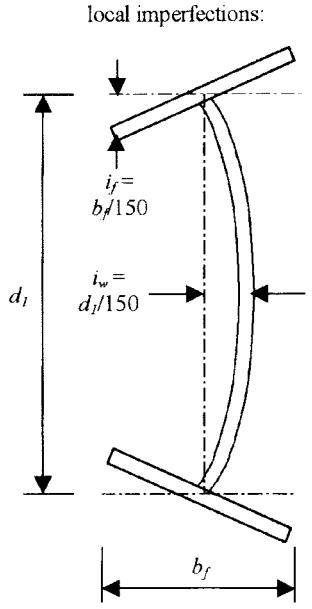

Fig. 2 Assumed local imperfections (SAA 1990)

scaling the appropriate buckling eigenvectors obtained from an elastic bifurcation buckling analysis of the model. The magnitudes of the local flange and web imperfections were taken as the assumed fabrication tolerances specified in AS4100 (SAA 1990) (see Fig. 2). The assumed residual stress distribution for hot-rolled I-sections (see Fig. 3) was recommended by ECCS (1984) and has been

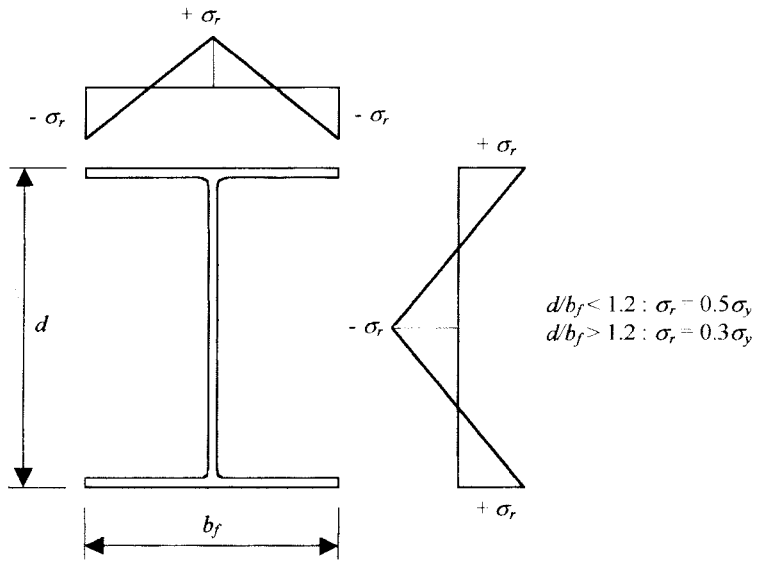

Fig. 3 Assumed longitudinal membrane residual stress distribution for hot-rolled I-sections (ECCS 1984)

adopted by numerous other researchers. The residual stresses were modelled using the Abaqus *INITIAL CONDITIONS option, with TYPE = STRESS, USER.

A concentrated nodal force and moment generating concentric axial compression and uniform major axis bending were applied at one end of the model. The force and moment were distributed using rigid surface R3D4 elements (see Fig. 1). These elements rigidly connected the translational degrees of freedom of all the nodes located on the end section to which the loads were applied, but did not in any way constrain the rotations or effect the local buckling deformations. Single point constraints were applied to all nodes located on the plane of symmetry to eliminate the translational degrees of freedom perpendicular to the plane and the rotational degrees of freedom about the axes defining the plane. These constraints ensured that the response of the model would be symmetrical, as required.

Elastic buckling analyses were conducted to determine the critical local buckling half wavelength, and to obtain the appropriate imperfection shape for each load combination. During preliminary analyses, it was observed that stress concentrations occurred due to the constraints caused by the rigid surface elements. These artificial stress concentrations adversely affected the stiffness reduction. The effects of the stress concentrations were eliminated by including a strip of elastic elements adjacent to the rigid surface at the load application end of the stub beam-column model (see Fig. 1).

2.2. Analytical results and discussion

Shell finite element stub beam-column models were developed for the three non-compact sections most frequently used in the analytical benchmark frame models used by Avery and Mahendran (1998b): the 310 UBi 32.0, 310 UBr1 32.0, and 310 UBr2 32.0 sections (see Table 1). Each section was analysed with pure major axis bending (i.e., $p = 0$), pure axial compression (i.e., $m = 0$), and 11 combinations of axial compression force and bending moment ($p/m = 0.02$, 0.05, 0.1, 0.2, 0.5, 1, 2,

Table 1 Section properties

Section	d (mm)	b_f (mm)	t_f (mm)	t_w (mm)	A_g (mm^2)	I (mm^4)	S (mm^3)	σ_y (MPa)
310 UBi 32.0	298	149	8.0	5.5	3979	6.131E+07	4.613E+05	320
310 UBr1 32.0	297	149	7.0	5.0	3536	5.403E+07	4.076E+05	370
310 UBr2 32.0	296	149	6.0	4.5	3093	4.674E+07	3.539E+05	420

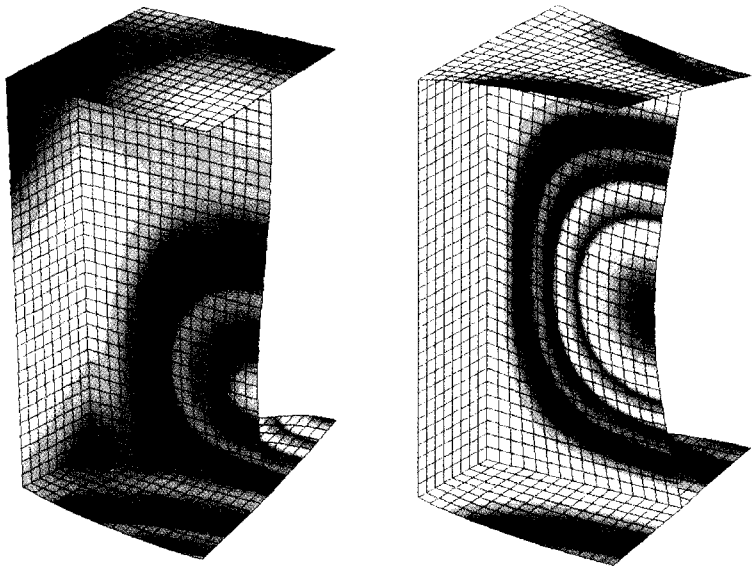

(a) pure bending (b) pure compression

Fig. 4 Local buckling modes

5, 10, 20, and 50). The deformed geometry and displacement contours corresponding to the ultimate load for the pure bending and pure axial compression load cases are illustrated in Fig. 4.

Three non-linear analyses were performed for each load case:

1. Second-order inelastic analysis with no local imperfections. The ultimate load factors for each load case were multiplied by the corresponding applied loads to obtain the plastic strength curve.
2. Second-order inelastic analysis with local imperfections. The ultimate load factors for each load case were multiplied by the corresponding applied loads to obtain the section capacity curve. Axial displacements (u_i) and major axis rotations (θ_i) were obtained for each load increment.
3. Second-order elastic analysis with local imperfections. The axial displacements (u_e) and major axis rotations (θ_e) were obtained for each load increment and subtracted from the corresponding inelastic deformations (u_i, θ_i) to derive the flexural tangent modulus (e_{tf}) and the axial tangent modulus (e_{ta}), as shown in Eq. (1). This procedure ensured that the section tangent moduli only included the effects of material yielding, as desired.

$$e_{tf}=\frac{\dot{\theta}_e}{\dot{\theta}_i};\quad e_{ta}=\frac{\dot{u}_e}{\dot{u}_i} \tag{1}$$

Table 2 Comparison of FEA and AS4100 effective section properties

Section	k_f		Z_e/S	
	FEA	AS4100	FEA	AS4100
310 UBi 32.0	0.890	0.902	0.980	0.976
310 UBr1 32.0	0.815	0.851	0.958	0.939
310 UBr2 32.0	0.719	0.802	0.894	0.887

The initial yield point for each load case was taken as the load at which the normalised tangent modulus corresponding to the dominant load dropped below 0.995. Stiffness reduction less than the 0.5 percent tolerance was assumed to be negligible.

2.2.1. Plastic strength, section capacity, and initial yield curves

The effective section ratios k_f and Z_e/S allow for the effects of local buckling through a reduction in cross-sectional area and section modulus in the case of axial compression and bending, respectively. The values obtained from the analyses of stub beam-column models are compared with the Australian steel structures code AS4100 (SA 1990) values for the 310 UBi 32.0, 310 UBr1 32.0, and 310 UBr2 32.0 sections in Table 2. The plastic strength, section capacity, and initial yield curves for one of the benchmark sections are provided in Fig. 5.

The analytical results indicated that:

- The AS4100 plastic strength equation is fairly accurate and generally conservative for hot-rolled I-sections subject to major axis bending and axial compression.
- The AS4100 section capacity equation and the AS4100 effective section properties are

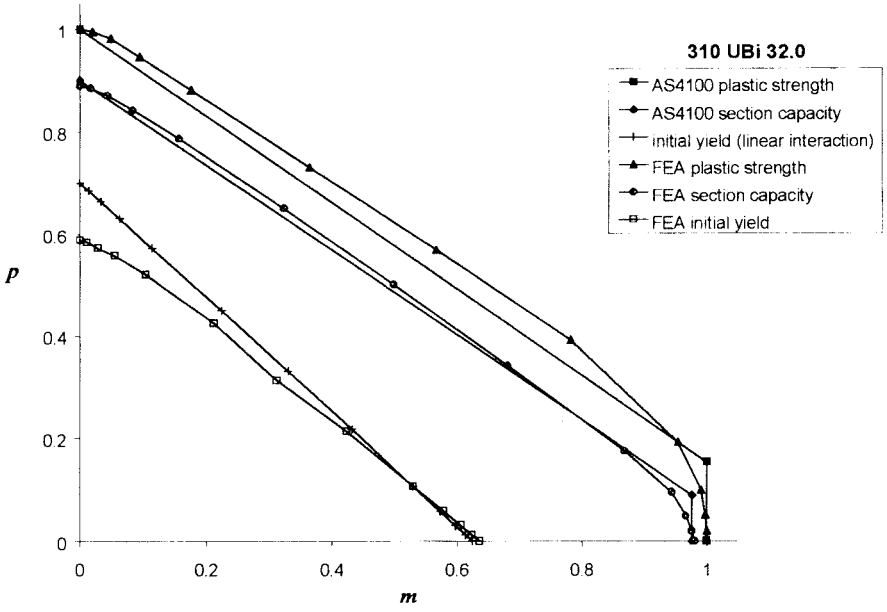

Fig. 5 Plastic strength, section capacity, and initial yield curves for the 310 UBi 32.0 section

reasonably accurate for the current range of hot-rolled I-sections (such as the 310 UBi 32.0). However, the AS4100 method significantly overestimates the section capacity of more slender sections (such as the 310 UBr2 32.0) for compression dominant load combinations. This trend is also indicated by comparison of the effective section properties (see Table 2), and can be attributed to the use of the maximum permitted local imperfection magnitude in the analytical model. The AS4100 section capacity is based on experimental testing of plate elements with more typical local imperfection magnitudes, and is therefore less conservative than the analytical model for slender sections whose capacities are sensitive to the imperfection magnitude.

- The initial yield point is influenced by the effects of local buckling, particularly for compression dominant load combinations. The linear interaction initial yield equation is therefore not appropriate for non-compact sections without suitable modification to account for the effects of local buckling.

2.2.2. Moment-curvature and axial compression force-strain curves

The normalised moment-curvature curves provided in Fig. 6 illustrate the gradual stiffness reduction and hinge softening behaviour of a typical non-compact hot-rolled I-section for a variety of different load combinations. Axial compression force-strain curves were also produced (Avery 1998).

Normalised moment-curvature curves for three different sections with varying slenderness are presented in Fig. 7 for the pure bending load case. It is clear that the rate of stiffness reduction and hinge softening is a function of the p/m ratio and the section slenderness. Furthermore, the rate of axial stiffness reduction differs from the rate of flexural stiffness reduction. Accurate and rational consideration of the effects of material inelasticity in non-compact sections therefore requires the use of two distinct flexural and axial tangent modulus functions. Each function must account for the effects of the p/m ratio and the section slenderness. The hinge softening model should also include the effects of the p/m ratio and the section slenderness. It should also be noted that the effects of flexural stiffness reduction and hinge softening are generally much more significant than the effects

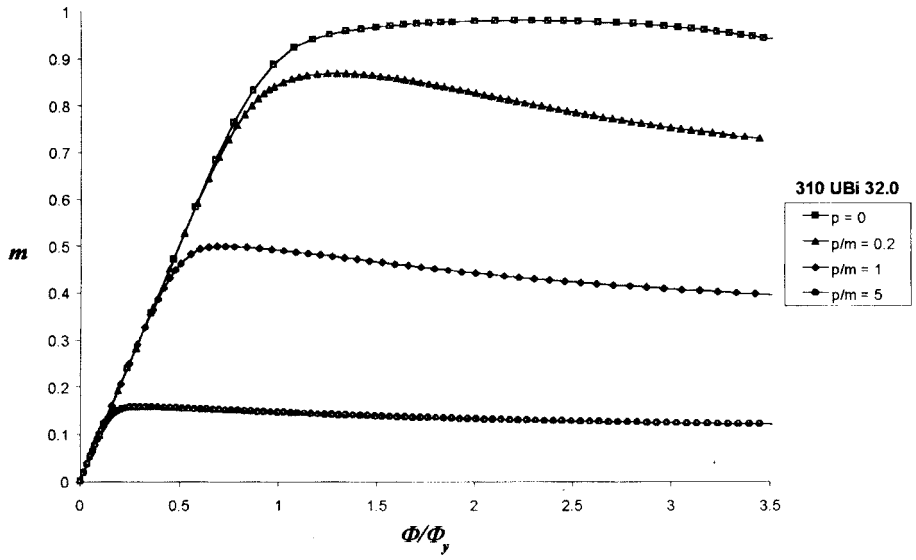

Fig. 6 Normalised moment-curvature curves

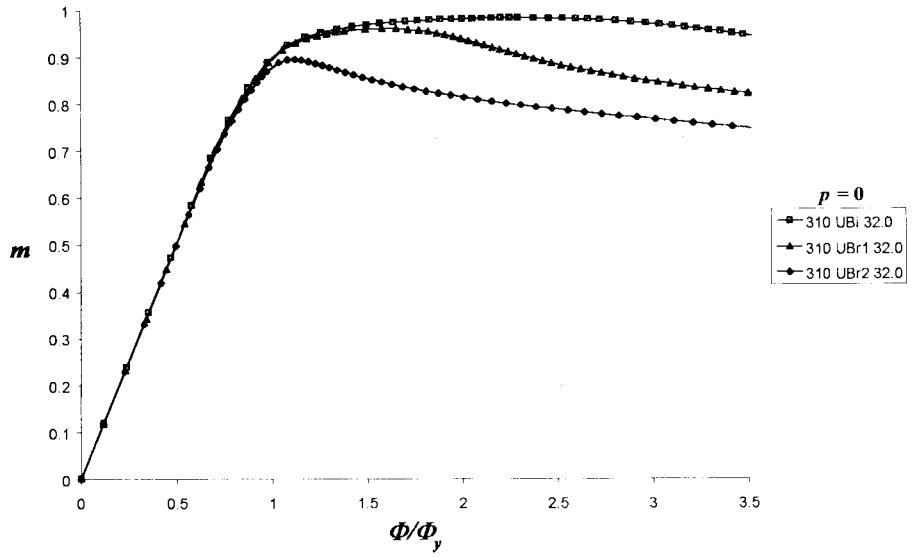

Fig. 7 Normalised moment-curvature curves showing the effect of section slenderness

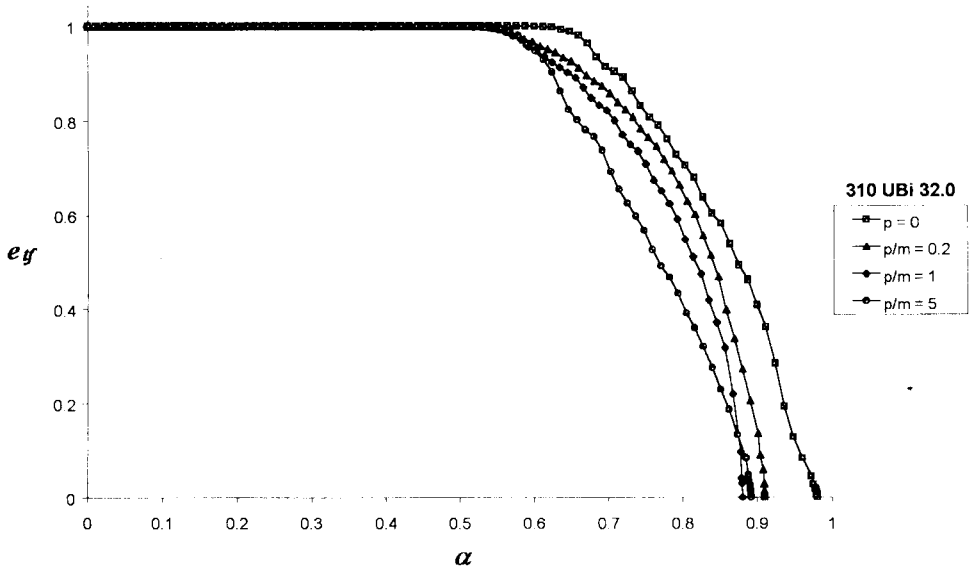

Fig. 8 Comparison of FEA flexural tangent modulus curves for four different p/m ratios

of axial stiffness reduction, as it is the reduction in flexural stiffness which initiates instability failure.

2.2.3. Tangent modulus curves

Flexural tangent modulus curves derived from the analytical results are presented in Figs. 8 and 9. Fig. 8 confirms the previous observation that the tangent modulus is a function of the p/m ratio. Fig. 9 illustrates the effect of section slenderness. The corresponding axial tangent modulus curves are

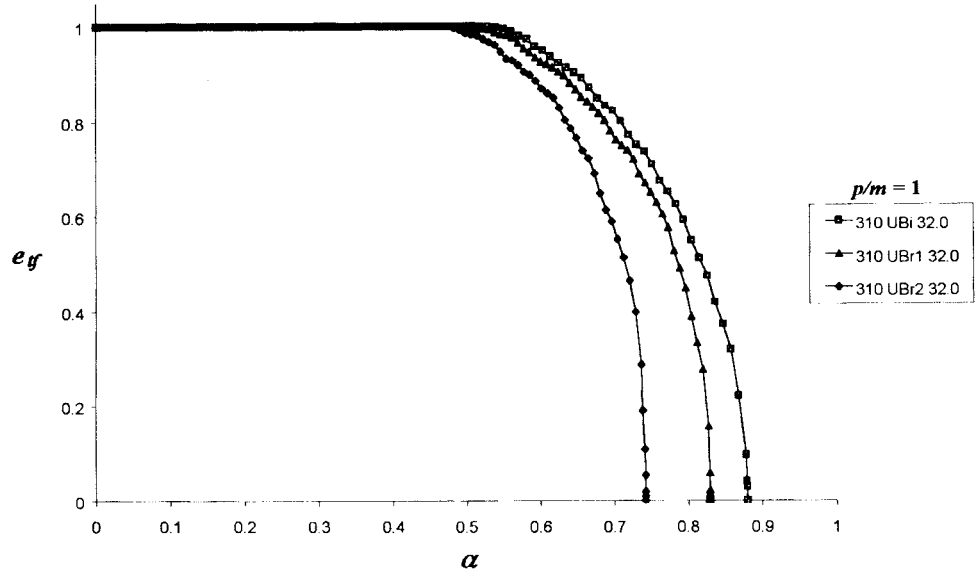

Fig. 9 Comparison of FEA flexural tangent modulus curves for three different section slendernesses

given in Avery (1998), which confirm the need for two distinct flexural and axial tangent modulus functions.

3. Formulation of the pseudo plastic zone frame element force-displacement relationship

The combined effects of material and geometric non-linearity can be represented by the following force-displacement relationship for a pseudo plastic zone frame element:

$$\begin{Bmatrix} \dot{M}_A \\ \dot{M}_B \\ \dot{P} \end{Bmatrix} = \frac{\zeta EI}{L} \begin{bmatrix} \phi_A \left[s_1' - \frac{s_2'^2}{s_1'}(1-\phi_B) \right] & \phi_A \phi_B s_2' & 0 \\ \phi_A \phi_B s_2' & \phi_B \left[s_1' - \frac{s_2'^2}{s_1'}(1-\phi_A) \right] & 0 \\ 0 & 0 & \frac{e_{ta} A}{\zeta I} \end{bmatrix} \begin{Bmatrix} \dot{\theta}_A \\ \dot{\theta}_B \\ u \end{Bmatrix} + \dot{f}_{lp} \tag{2}$$

The formulation of the pseudo plastic zone force-displacement relationship is similar to the refined plastic hinge formulation described by Avery and Mahendran (1998a) and Liew (1992). However, several significant differences exist.

1. The plastic strength, section capacity, initial yield, tangent modulus, and hinge softening equations for the pseudo plastic zone formulation are accurately determined from the results of the stub beam-column model analyses. The refined plastic hinge formulation uses approximate

equations based on the AS4100 (1990) or AISC LRFD (1995) specification equations.

2. The pseudo plastic zone method's tangent modulus represents the reduction in stiffness due only to gradual yielding for a particular *section* and applied load combination of axial force and bending moment. It does not include any approximate implicit consideration of member instability and member imperfections, as is the case for the refined plastic hinge formulation. These effects are dealt with in isolation using inelastic stability functions (s'_1, s'_2) and a new imperfection reduction factor (ζ), respectively. Isolation of the two effects enables a more rational and accurate representation.

3. The pseudo plastic zone formulation includes separate tangent modulus functions for flexural and axial stiffness (E_{tf}, E_{ta}). The stiffness reduction due to initial member imperfections is only applied to the flexural stiffness term, as the imperfections have negligible influence on the axial stiffness. The refined plastic hinge formulation uses a single tangent modulus (including the effects of initial imperfections) for both flexural and axial stiffness reductions.

4. The pseudo plastic zone's flexural stiffness reduction parameters (ϕ_A, ϕ_B) are evaluated directly from the flexural tangent modulus, and replace the flexural tangent modulus in the force-displacement relationship. In the refined plastic hinge model, the tangent modulus is used in combination with the flexural stiffness reduction parameters, often resulting in an overestimation of the total stiffness reduction.

Note that the pseudo plastic zone structure force-displacement relationship can be assembled and solved using the same procedure as the refined plastic hinge method (Avery and Mahendran 1998a, Liew 1992).

3.1. Plastic strength, section capacity and initial yield

The normalised plastic strength can be conveniently defined as a function of the p/m ratio using a series of cubic equations in the following form:

$$p_{ps}=a_0+a_1t+a_2t^2+a_3t^3; \quad m_{ps}=\frac{p_{ps}}{p/m}; \quad t=\tan^{-1}(p/m) \tag{3}$$

The variable t represents the angle between the horizontal m axis and the line representing the load path OA from the origin O(0, 0) to the applied load point A(m, p) on the m-p interaction diagram (Fig. 10). As t varies from zero to $\pi/2$, it is a preferable regression variable to the p/m ratio which varies from zero to infinity. Furthermore, because t is a simple function of the p/m ratio, the plastic strength corresponding to any applied loads can be directly evaluated from Eq. (3) without solving a polynomial equation as is required for alternative functions such as those proposed by Duan and Chen (1990) and Attalla *et al.* (1994).

The constants a_0, a_1, a_2, and a_3 were determined from a least squares regression analysis of the stub beam-column model results for each section. The plastic strength is independent of the section slenderness, therefore the same plastic strength constants can be used for benchmark sections 310 UBi 32.0, 310 UBr1 32.0, and 310 UBr2 32.0. These constants are provided in Table 3.

The normalised section capacity of members subject to pure bending (i.e., $p = 0$) or pure axial compression (i.e., $m = 0$), the section capacity can be calculated directly from the effective section properties (k_f, Z_e/S) obtained from the stub beam-column analyses.

$$\text{for } p = 0\text{: } m_{sc} = Z_e/S$$

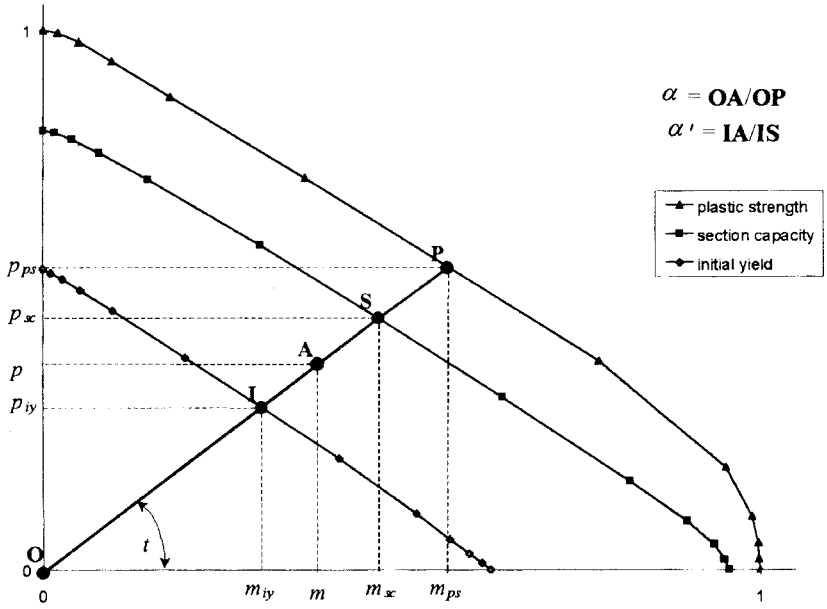

Fig. 10 *m-p* interaction diagram

Table 3 Plastic strength constants for the 310 UBi 32.0, 310 UBr1 32.0, and 310 UBr2 32.0 sections

	a_0	a_1	a_2	a_3
$p/m < 0.2$	0.0000	0.9980	0.0766	−1.1950
$0.2 < p/m < 5$	−0.0032	1.1095	−0.6814	0.2494
$p/m > 5$	52.2780	−106.9742	73.7485	−16.8247

$$\text{for } m = 0\text{: } p_{sc} = k_f \tag{4}$$

The normalised section capacity of a member subject to combined bending and axial compression can be defined in similar fashion to the plastic strength:

$$p_{sc}=b_0+b_1t+b_2t^2+b_3t^3; \quad m_{sc}=\frac{p_{sc}}{p/m}; \quad t=\tan^{-1}(p/m) \tag{5}$$

The constants b_0, b_1, b_2, and b_3 were determined from a least squares regression analysis for each section. These constants are provided in Table 4 for the 310 UBi 32.0 section. Constants for the other sections are provided by Avery (1998).

It is to be noted that Eqs. (3) and (5) are not used for the limiting cases of $m = 0$ and $p = 0$, instead the limiting values of 1 for m_{ps} and p_{ps}, and effective section properties of Z_e/S and k_f for m_{sc} and p_{sc} as in Eq. (4) are used.

The initial yield of a non-compact section can be defined using a modified linear interaction equation:

$$p_{iy}=\frac{k_f(1-\sigma_r/\sigma_y)}{1+\dfrac{k_f}{Z/S}\dfrac{1}{p/m}}; \quad m_{iy}=\frac{p_{iy}}{p/m} \tag{6}$$

Table 4 Section capacity constants for the 310 UBi 32.0 section

	b_0	b_1	b_2	b_3
$p/m < 0.2$	0.0000	0.9789	−0.1302	−1.8883
$0.2 < p/m < 5$	0.0186	0.8709	−0.4643	0.1727
$p/m > 5$	16.0194	−32.5776	22.8440	−5.2423

Eq. 6 is based on the conventional linear interaction equation, which has been used by other researchers (Attalla *et al.* 1994) for compact sections. The effect of section slenderness on the initial yield is accounted for by using the analytical form factor (k_f) to reduce the normalised axial force axis intercept.

The approximate plastic strength, section capacity, and initial yield curves obtained using Eqs. (3), (5), and (6) are compared with the analytical results in Fig. 11 for the 310 UBi 32.0 section. This figure shows that the equation lines provide an accurate approximation of the analytical result points.

3.2. Section tangent moduli

The normalised axial and flexural tangent modulus functions for the pseudo plastic zone formulation are defined using Eq. (7):

$$e_t = 1 - c_1 \alpha'^{c_2} - (1 - c_1)\alpha'^{c_3} \tag{7}$$

A variety of different equation forms were investigated. Eq. (7) was found to be the most appropriate function, with sufficient flexibility to accurately trace all of the tangent modulus

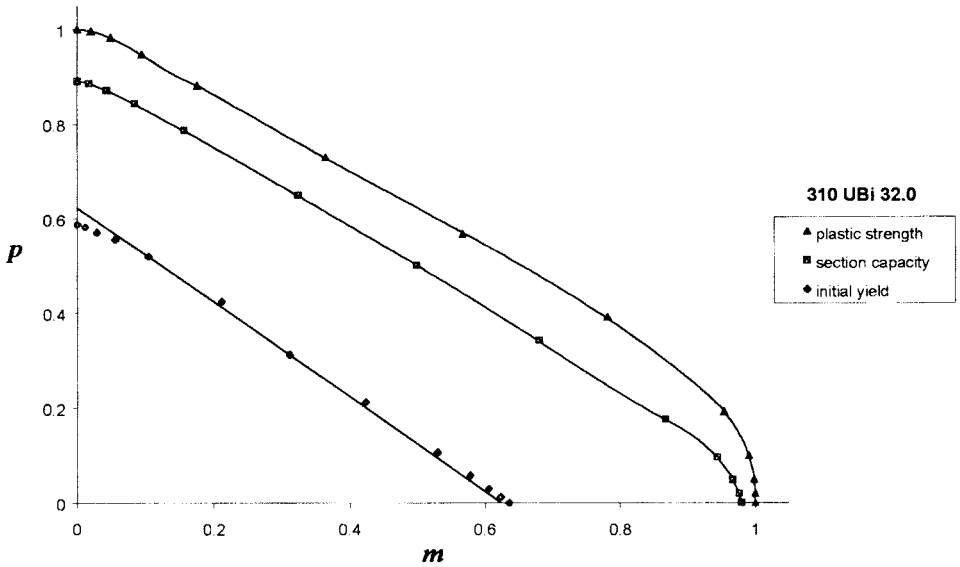

Fig. 11 Comparison of FEA and approximate plastic strength, section capacity, and initial yield equations for the 310 UBi32 Section

Table 5 Tangent modulus constants for the 310 UBi 32.0 section

Load combination	Flexural			Axial		
	c_1	c_2	c_3	c_1	c_2	c_3
$p = 0.00$	0.447	1.023	2.735	0.658	0.328	3.185
$p/m = 0.02$	0.679	1.379	4.473	0.658	0.328	3.185
$p/m = 0.05$	0.795	1.689	9.063	0.658	0.328	3.185
$p/m = 0.10$	0.751	1.809	7.800	0.612	0.573	1.082
$p/m = 0.20$	0.528	1.449	6.866	0.322	1.271	1.014
$p/m = 0.50$	0.620	1.560	12.229	0.721	1.277	8.529
$p/m = 1.00$	0.685	1.624	20.140	0.631	1.711	19.319
$p/m = 2.00$	0.697	1.244	12.868	0.520	1.749	20.906
$p/m = 5.00$	0.847	1.011	11.972	0.557	2.235	40.345
$p/m = 10.0$	0.923	0.839	10.784	0.622	2.439	84.784
$p/m = 20.0$	0.976	0.772	307.333	0.656	2.363	88.556
$p/m = 50.0$	0.990	0.745	307.333	0.690	2.341	74.103
$m = 0.00$	0.990	0.745	307.333	0.585	1.828	17.028

functions obtained from the stub beam-column analyses. Eq. (7) is a simple polynomial decay function, containing a lower order (c_2) term, a higher order (c_3) term, and a weighting parameter (c_1) to vary the relative significance of the lower order and higher order terms.

The tangent modulus is conveniently defined as a function of the effective plastic force state parameter (α'), which can be evaluated using Eq. (8). The effective plastic force state parameter varies from zero at the point of initial yield, to one when the section capacity is reached. The relationship between the force state parameter (α) and the effective force state parameter (α') is illustrated on the *m-p* interaction diagram (Fig. 10). As shown in Fig. 10, α' = IA/IS, while α = OA/OP.

$$\alpha' = 0 \quad \text{for } \alpha \leq \alpha_{iy}$$

$$\alpha' = \frac{(\alpha - \alpha_{iy})}{(\alpha_{sc} - \alpha_{iy})} \quad \text{for} \quad \alpha > \alpha_{iy} \tag{8}$$

The constants c_1, c_2, and c_3 were determined by a least-squares regression analysis for each section and load combination. Tangent moduli for intermediate p/m ratios can be evaluated using linear interpolation, using $\tan^{-1}(p/m)$ as the interpolation variable. Values of c_1, c_2, and c_3 for the 310 UBi 32.0 section are provided in Table 5. Values for the other sections are provided by Avery (1998). The approximate flexural and axial tangent modulus curves obtained using Eq. (7) are compared with the analytical results in Fig. 12 for one of the load combinations.

3.3. Hinge softening

The reduction in the section capacity and stiffness due to hinge softening can be approximately modelled by replacing the tangent modulus with a negative softening modulus after the formation of a plastic hinge (i.e., $e_{tf} = e_s$). The normalised flexural softening modulus (e_s) can be determined from the analytical moment-curvature curves for each section and load combination. These curves

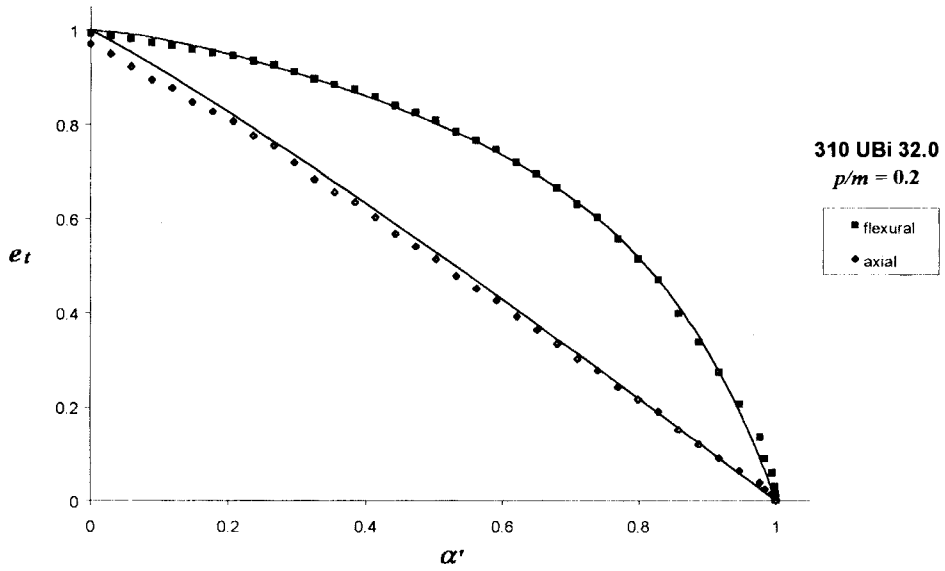

Fig. 12 Comparison of the approximate and FEA tangent modulus curves (310 UBi 32.0 section, $p/m = 0.2$)

Table 6 Normalised flexural softening moduli for the 310 UBi 32.0 section

Load combination	Softening modulus (e_s)	Load combination	Softening modulus (e_s)
$p = 0.00$	− 0.0472	$p/m = 2.00$	− 0.0957
$p/m = 0.02$	− 0.0521	$p/m = 5.00$	− 0.1025
$p/m = 0.05$	− 0.0590	$p/m = 10.0$	− 0.1051
$p/m = 0.10$	− 0.0701	$p/m = 20.0$	− 0.1089
$p/m = 0.20$	− 0.0793	$p/m = 50.0$	− 0.1088
$p/m = 0.50$	− 0.0834	$m = 0.00$	− 0.1088
$p/m = 1.00$	− 0.0885		

indicate that the initial rate of hinge softening is reasonably constant for plastic curvatures within the range that may occur in typical steel frame structures. The flexural softening moduli can therefore be conservatively calculated from the slope of lower bound tangent to the moment-curvature curves.

Softening modulus values for the 310 UBi 32.0 section are provided in Table 6 for each load combination. Values for the other sections are provided by Avery (1998). Softening moduli for intermediate p/m ratios can be evaluated using linear interpolation, using $\tan^{-1}(p/m)$ as the interpolation variable.

3.4. Imperfection reduction factor

It is desirable to avoid explicit modelling of member out-of-plumbness and out-of-straightness imperfections in a concentrated plasticity advanced analysis. The refined plastic formulation relies on the reduced tangent modulus function to provide the necessary stiffness reduction to implicitly account for member imperfections. This approach does not allow for the effects of the vertical to

horizontal load ratio, initial imperfection magnitude, and total deflection on the magnitude of the stiffness reduction. The first-order slope-deflection functions and equations of equilibrium can be used to derive an improved stiffness reduction function for a sway beam-column member (Avery 1998):

$$\zeta = \frac{\left(1 + \frac{P}{H}\frac{\Delta}{L}\right)}{\left(1 + \frac{P}{H}\frac{(\Delta_i + \Delta)}{L}\right)} \tag{9}$$

Although the derivation of Eq. (9) is based on a sway member, the equation can also be used for non-sway members, provided a minimum of two elements per member are used. The free body diagram of an element defining half the length of a non-sway member is in fact identical to that of the sway beam-column member used to derive Eq. (9). The imperfection stiffness reduction factor (ζ) accounts for the following:

- The vertical to horizontal load ratio (P/H). In a frame analysis, the stiffness reduction factor is calculated for each individual element. The vertical load (P) is taken as the magnitude of the element axial compression force, while the horizontal load (H) is taken as the magnitude of the element shear force. The vertical load is taken as zero for tension members. Elements with zero shear (i.e., $H = 0$) require explicit modelling of member imperfections. Eq. (9) indicates a decrease in ζ with increasing P/H ratios.
- The initial imperfection magnitude (Δ_i). The recommended ratio of the initial imperfection magnitude to element length (Δ_i/L) is 1/500 for both sway and non-sway members. Note that the ratio of imperfection magnitude to *element* length is double the ratio of imperfection magnitude to *member* length for non-sway members with at least two elements per member. Eq. (9) indicates a decrease in ζ with increasing Δ_i/L ratios.
- The total deflection (Δ). The effect of the initial imperfection diminishes as the total deflection

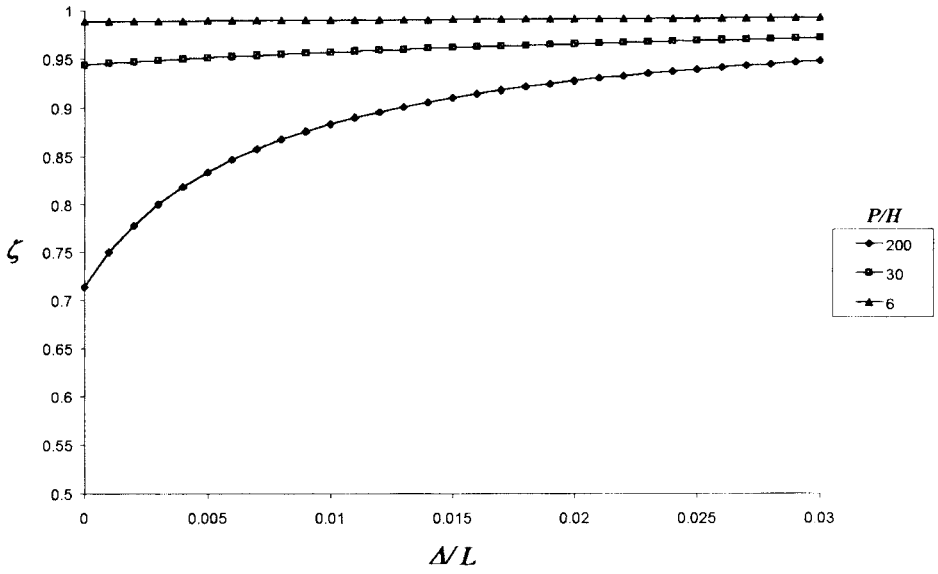

Fig. 13 Imperfection reduction factor vs. normalised total displacement for various element P/H ratios and Δ_i/L = 1/500

increases. In a frame analysis, the total deflection is taken as the relative deflection of the element nodes at the end of the previous load increment. The initial stiffness reduction can be determined by taking $\Delta = 0$.

The imperfection reduction function is illustrated in Fig. 13 for $\Delta_i/L = 1/500$ and three P/H ratios. This Figure suggests that the constant 0.877 imperfection reduction factor used in the AISC LRFD compression member capacity equations is unconservative for members with high P/H ratios and smaller total displacements, and conservative for members with low P/H ratios. Note that the element axial force to shear force P/H ratio is approximately double the applied load P/H ratio for a single storey, single bay sway frame.

It is to be noted that this study considers only a proportional loading as it is generally adequate for incremental solution procedures, and preferable for practical advanced analysis. Analytical results indicate that non-proportional loading is slightly more conservative than proportional loading for typical frame configurations and load cases (Avery 1998).

3.5. Second-order effects

Accurate consideration of the second-order instability of an inelastic beam-column member would require the solution of a second-order differential equation with non-constant coefficients:

$$E_{tf}I(\dot{y})'' + P\dot{y} = \frac{\dot{M}_A + \dot{M}_B}{L}x - \dot{M}_A \tag{10}$$

After the commencement of yielding, the flexural tangent modulus (E_{tf}) will vary along the length of the member. It is therefore not possible to obtain a simple closed-form solution to Eq. 10. An approximate solution can be obtained by using:

- Inelastic stability functions (s'_1, s'_2) calculated using the mean flexural tangent modulus (E'_{tf}) instead of the elastic modulus, as shown in Eqs. 11 and 12. The simplified expressions for the stability functions shown in these equations are as proposed by Lui and Chen (1986).
- A flexural stiffness reduction function based on the tangent moduli at the element ends to account for the longitudinal distribution of plasticity.

$$s_1' = 4 + \frac{2\pi^2\rho'}{15} - \frac{(0.01\rho' + 0.543)\rho'^2}{4 + \rho'} + \frac{(0.004\rho' + 0.285)\rho'^2}{8.183 + \rho'}$$

$$s_2' = 2 - \frac{\pi^2\rho'}{30} + \frac{(0.01\rho' + 0.543)\rho'^2}{4 + \rho'} - \frac{(0.004\rho' + 0.285)\rho'^2}{8.183 + \rho'} \tag{11}$$

where:

$$\rho' = \frac{PL^2}{\pi^2 E_{tf}' I} \tag{12}$$

Note that a tensile axial force (P) is taken as positive in Eq. (12).

This approximate solution will converge to the true solution as the number of elements per member is increased. However, two elements per member were found to provide adequate results. Note that the mean flexural tangent modulus (E'_{tf}) can be taken as the average of the flexural tangent moduli calculated at the element ends (E_{tfA}, E_{tfB}), as shown in Eq. (13).

$$E_{tf}'=\frac{E_{tfA}+E_{tfB}}{2} \tag{13}$$

3.6. Flexural stiffness reduction parameter

The flexural stiffness reduction factor (ϕ) can be calculated directly from the flexural tangent modulus using Eq. (14):

$$\phi=(0.5-1/\beta)+\frac{\beta}{|\beta|}\sqrt{(0.5-1/\beta)^2+2e_{tf}/\beta} \quad \text{for} \quad \beta\neq 0$$

$$\phi=e_{tf} \quad \text{for} \quad \beta=0 \tag{14}$$

A derivation of Eq. (14) is provided by Avery (1998). The end moment ratio (β) is defined as:

$$\beta=\frac{M_A}{M_B};\quad |M_A|<|M_B|;\quad -1\leq\beta\leq 1 \tag{15}$$

4. Verification of the pseudo plastic zone analytical method

A series of 102 benchmark analyses of single bay, single storey, sway portal frames comprising non-compact I-sections subject to major axis bending was presented by Avery and Mahendran (1998b). The benchmark frames included fixed base, pinned base, and leaned column frames with different loading. In order to establish the validity, accuracy and reliability of the pseudo plastic zone method for the analysis of steel frames comprising non-compact sections, a selection of these benchmark frames were analysed using the new model. In this section, the results of these pseudo plastic zone analyses are compared with the finite element analytical benchmark solutions.

These benchmark solutions were obtained using a distributed plasticity shell finite element model of the portal frame (Avery and Mahendran 1998c) that was verified by comparison with the experimental results of frames comprising non-compact sections (Avery and Mahendran 1998d) and a variety of analytical benchmarks comprising compact sections (Vogel 1985). The verification analyses indicated that the distributed plasticity shell finite element model is accurate and reliable for second-order inelastic analysis of steel frame structures comprising non-compact sections. Therefore the analytical benchmark solutions developed from this model are also considered accurate and reliable and can be used to verify the accuracy of simplified concentrated plasticity methods of advanced analysis such as the one described in this paper. It is noted that currently no other benchmark solutions are available for non-compact sections.

The results of the pseudo plastic zone analyses are also compared with Avery and Mahendran's (1998a) refined plastic hinge solutions, and the specification design capacities. All of the results are compared using tabulated summaries of ultimate load capacities, normalised strength curves, and load-deflection curves. A representative selection of these tables and charts is presented in this section, while a more comprehensive presentation of all results and comparisons is provided by Avery (1998).

As stated in previously, stub beam-column analyses were only conducted for the 310 UB 32.0 sections. Model parameters (e.g., the section capacity and tangent modulus coefficients) were therefore only obtained for these sections. This limited the range of benchmark frames that could be analysed with the pseudo plastic zone model.

The pseudo plastic zone sway load-deflection curves (PPZ) for two of the fixed base portal frames

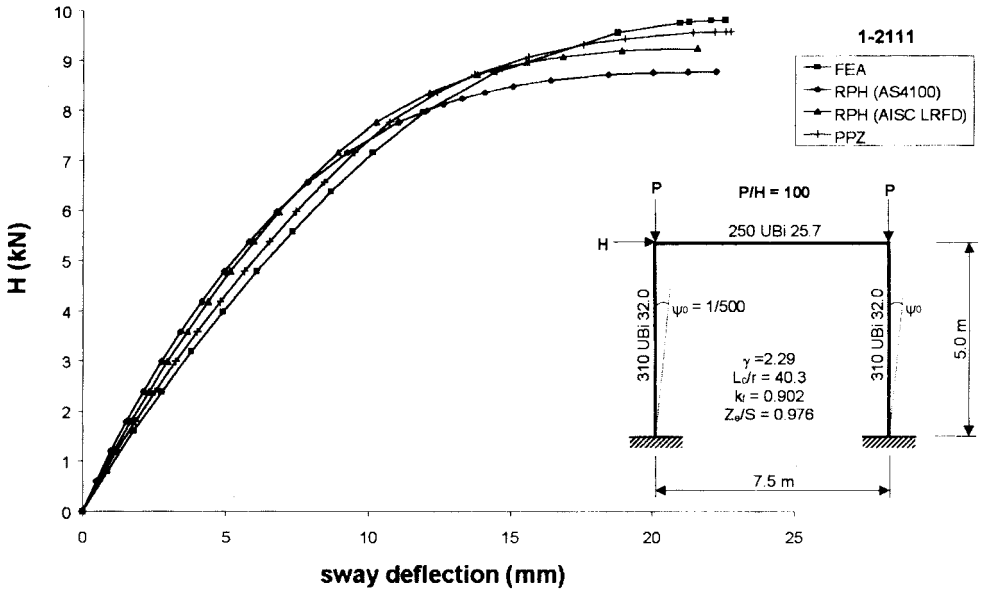

Fig. 14 Sway load-deflection curves for benchmark frame 1-2111

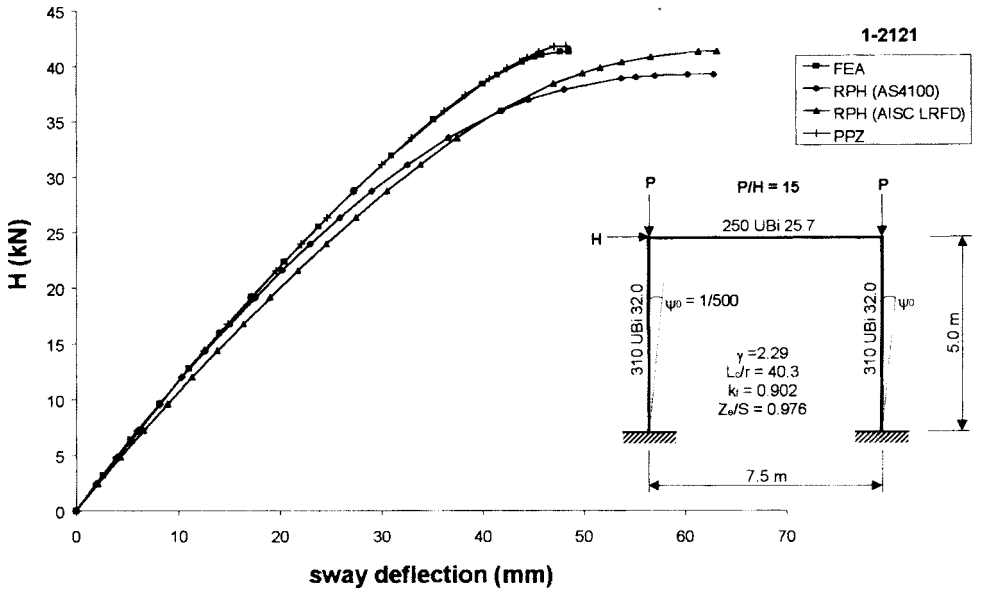

Fig. 15 Sway load-deflection curves for benchmark frame 1-2121

are illustrated in Figs. 14 and 15, and compared with the exact finite element benchmark solutions (FEA) and Avery and Mahendran's (1998a) refined plastic hinge solutions using AS4100 specification (RPH-AS4100) and AISC LRFD specification (RPH-AISC LRFD).

Based on the results of the benchmark analyses, the following observations can be made regarding the performance of the pseudo plastic zone (PPZ) model:

1. The initial flexural stiffness is more accurately modelled in the pseudo plastic zone method

compared with the refined plastic hinge methods, justifying the applicability of Eq. (9) (see Figs. 14 and 15). The initial stiffness is still slightly overestimated for frames with high *P/H* ratios, but this does not appear to adversely effect the accuracy of the model.

2. For frames with larger *P/H* ratios as in Fig. 14, the difference in the initial stiffness is due to the different approaches used in modelling the initial out-of-plumbness imperfections. In the refined plastic hinge method (RPH), an approximate constant reduction factor of 0.85 is used, and does not take into account the fact that the *P/H* ratio significantly influences the initial stiffness reduction due to imperfections. For frames with larger *P/H* ratios, the imperfection and associated displacements are significant compared with the small overall sway displacements. Eq. (9) of the pseudo plastic zone method (see also Fig. 13) takes this into account and the PPZ initial stiffness is therefore much closer to the FEA solution than the RPH method. If an analysis of a frame with no imperfection is conducted, the PPZ method would match the linear elastic solution because the imperfection stiffness reduction factor is a function of the initial imperfection magnitude and reduces to 1.0 when $\Delta_i = 0$.

3. The rate of stiffness reduction is more accurately modelled in the pseudo plastic zone method compared with the refined plastic hinge methods, evidenced by the close agreement between the pseudo plastic zone and finite element benchmark load-deflection curves and ultimate loads (Figs. 14 and 15). This justifies the use of the section tangent moduli (Eq. 7), flexural stiffness reduction function (Eq. 14), and inelastic stability functions (Eq. 11) to model the gradual stiffness reduction due to yielding and the associated second-order effects.

4. The load-deflection curves (Figs. 14 and 15) indicate that the initial yield point is accurately modelled, justifying the applicability of the pseudo plastic zone method initial yield function (Eq. 6).

5. The pseudo plastic hinge model does not appear to overestimate the inelastic redistribution ductility, as occurred in the refined plastic hinge model (Avery and Mahendran 1998a). This suggests that the simplified constant hinge softening modulus approach is suitably accurate if the appropriate modulus is used.

6. The consistent accuracy of the pseudo plastic zone method also demonstrates the accuracy of the section capacity equation (Eq. 5) derived from the stub beam-column models.

7. The axial stiffness is more accurately modelled in the pseudo plastic zone method compared with the refined plastic hinge method due to the use of separate flexural and axial tangent moduli.

A comparison between the ultimate loads obtained from the pseudo plastic zone (PPZ) analyses, benchmark finite element analysis (FEA), refined plastic hinge (RPH) analyses, and specification design calculations is summarised in Table 7.

The pseudo plastic zone method is suitable for all of the benchmark frame types investigated in this study. The method is significantly more accurate and precise than both the conventional individual member design methods based on elastic analysis and specification equations, and the refined plastic hinge methods. On average, the pseudo plastic zone model is 1% conservative, with an acceptable maximum unconservative error of 4.9 percent. The pseudo plastic zone model can allow the design capacity to be increased by up to 29.0 percent for simple frames, mainly due to the consideration of inelastic redistribution (Avery 1998).

The results presented in this paper have been limited to a series of 310 UB 32 sections. However, the paper has provided the analytical framework and other essential details to enable its application to other UB sections or cross-sections. Recently, Yuan *et al.* (1999) has extended the work described in this paper to include the current range of Australian hot-rolled UB sections.

Table 7 Summary of benchmark analysis results

	Mean	Coefficient of variation	Maximum	Minimum
PPZ / FEA	0.990	0.023	1.049	0.941
RPH (AS4100) / FEA	0.945	0.047	1.066	0.864
RPH (AISC) / FEA	1.009	0.064	1.165	0.869
PPZ / RPH (AS4100)	1.048	0.037	1.113	0.944
PPZ / RPH (AISC)	0.983	0.059	1.119	0.833
PPZ / Design (AS4100)	1.105	0.069	1.290	0.944
PPZ / Design (AISC)	1.071	0.052	1.194	0.920

5. Conclusions

A concentrated plasticity model for the advanced analysis of steel frame structures has been presented in this paper. This pseudo plastic zone model accounts for the effects of local buckling using the tangent moduli, section capacity, and initial yield equations derived from distributed plasticity finite element analysis of a stub beam-column model. The accuracy and precision of the new model has been extensively verified using the analytical benchmarks presented by Avery and Mahendran (1998b).

Acknowledgements

The authors wish to thank QUT for providing financial support through the QUT Postgraduate Research Award (QUTPRA) and the 1996 Meritorius Research Project Grants Scheme, and the Physical Infrastructure Centre and the School of Civil Engineering at QUT for providing the necessary facilities and support to conduct this project.

References

AISC (1995), *Manual of Steel Construction, Load and Resistance Factor Design*, 2nd Ed., American Institute of Steel Construction, Chicago, IL, USA.

Attalla, M.R., Deierlein, G.G. and McGuire, W. (1994), "Spread of plasticity: quasi-plastic-hinge approach", *Journal of Structural Engineering, ASCE*, **120**(8), 2451-2473.

Avery, P. (1998), "Advanced analysis of steel frames comprising non-compact sections", Ph.D. thesis, School of Civil Engineering, Queensland University of Technology, Brisbane, Australia.

Avery, P. and Mahendran, M. (1998a), "Refined plastic hinge analysis of steel frame structures comprising non-compact sections", Physical Infrastructure Centre Research Monograph 98-4, Queensland University of Technology, Brisbane, Australia.

Avery, P. and Mahendran, M. (1998b), "Analytical benchmark solutions for steel frame structures comprising non-compact sections", Physical Infrastructure Centre Research Monograph 98-3, Queensland University of Technology, Brisbane, Australia, Also in *International Journal of Advances in Structural Engineering*, In print.

Avery, P. and Mahendran, M. (1998c), "Distributed plasticity analysis of steel frame structures comprising non-compact sections", *Physical Infrastructure Centre Research Monograph 98-2*, Queensland University of Technology, Brisbane, Australia, *Also in Engineering Structures*, **20**(8), 2000, in print

Avery, P. and Mahendran, M. (1998d), "Large scale experiments of steel frame structures comprising non-compact sections", *Physical Infrastructure Centre Research Monograph 98-1, Queensland University of Technology, Brisbane, Australia, Also in Engineering Structures*, **20**(8), 2000, In print.
Duan, L. and Chen, W.F. (1990), "A yield surface equation for doubly symmetric sections", *Engineering Structures*, **12**, 114-119.
ECCS (1984), "Ultimate limit state calculation of sway frames with rigid joints", *Technical Committee*, 8, publication No. 33.
HKS (1997), *Abaqus User's Manual*, Hibbitt Karlsson & Sorensen, Pawtucket, U.S.A.
King, W.S. and Chen, W.F. (1994), "Practical second-order inelastic analysis of semi-rigid frames", *Journal of Structural Engineering, ASCE*, **120**(7), 2156-2175.
Liew, J.Y.R. (1992), "Advanced analysis for frame design", PhD dissertation, School of Civil Engineering, Purdue University, West Lafayette, IN, U.S.A.
Liew, J.Y.R., White, D.W. and Chen, W.F. (1993), "Second-order refined plastic-hinge analysis for frame design. Parts I&II", *Journal of Structural Engineering, ASCE*, **119**(11), 3196-3237.
Lui, E.M. and Chen, W.F. (1986), "Analysis and behaviour of flexibly-jointed frames", *Engineering Structures*, **8**, 107-118.
Vogel, U. (1985), "Calibrating frames", *Stahlbau*, **54**, 295-301.
SA (1990), "AS4100-1990 Steel Structures", Standards Australia, Sydney, Australia.
Yuan, Z., Mahendran, M. and Avery, P. (1999), "A parametric study of non-compact i-sections for the pseudo plastic zone analysis method", *Physical Infrastructure Centre Research Monograph* 99-4, Queensland University of Technology, Brisbane, Australia.

Notation

A_g = gross cross-section area
a_i = constant used to define the plastic strength
b_i = constant used to define the section capacity
b_f = flange width
c_i = constant used to define the tangent modulus
d = total depth of section
d_1 = clear depth of web
E = elastic modulus
e_s = non-dimensional softening modulus = E_s/E
E_s = softening modulus
e_t = non-dimensional tangent modulus = E_t/E
E_t = tangent modulus
E_{ta} = axial tangent modulus
e_{ta} = non-dimensional axial tangent modulus = E_{ta}/E
E_{tf} = flexural tangent modulus
E_{tfA}, E_{tfB} = flexural tangent modulus at element ends A and B
E'_{tf} = mean flexural tangent modulus
e_{tf} = non-dimensional flexural tangent modulus = E_{tf}/E
$\boldsymbol{f}_{lp}$ = local element pseudo-force vector
H = applied horizontal load
I = second moment of area with respect to the axis of in-plane bending
I_b = second moment of area of beam section
I_c = second moment of area of column section
k_f = form factor for axial compression member
L = member length or length of element chord
L_b = length of beam member
L_c = length of column member

M = bending moment
m = non-dimensional bending moment = M/M_p
M_A, M_B = bending moment at element ends A and B
M_{iy} = bending moment defining the initial yield
m_{iy} = non-dimensional bending moment defining the initial yield = M_{iy}/M_p
M_p = plastic moment capacity = $\sigma_y S$
M_{ps} = bending moment defining the plastic strength
m_{ps} = non-dimensional bending moment defining the plastic strength = M_{ps}/M_p
M_{sc} = bending moment defining the section capacity
m_{sc} = non-dimensional bending moment defining the section capacity = M_{sc}/M_p
P = axial force or applied vertical load
p = non-dimensional axial force = P/P_y
P_{iy} = axial force defining the initial yield
p_{iy} = non-dimensional axial force defining the initial yield = P_{iy}/P_y
P_{ps} = axial force defining the plastic strength
p_{ps} = non-dimensional axial force defining the plastic strength = P_{ps}/P_y
P_{sc} = axial force defining the section capacity
p_{sc} = non-dimensional axial force defining the section capacity = P_{sc}/P_y
P_y = squash load = $\sigma_y A_g$
S = plastic section modulus with respect to the axis of in-plane bending
s_1', s_2' = inelastic stability functions
t = variable used to define the plastic strength and section capacity
t_f, t_w = flange and web thicknesses
u = axial displacement
u_e = axial displacement from elastic analysis
u_i = axial displacement from inelastic analysis
x = distance along member from end A
y = in-plane transverse displacement at location x
Z = elastic section modulus with respect to the axis of in-plane bending
Z_e = effective section modulus with respect to the axis of in-plane bending
Δ = relative lateral deflection between element ends
Δ_i = initial imperfection magnitude
Φ = curvature
α' = effective force state parameter
α = force state parameter
α_{iy} = force state parameter corresponding to initial yield
α_{sc} = force state parameter corresponding to section capacity
β = end moment ratio
ϕ = flexural stiffness reduction factor
ϕ_A, ϕ_B = flexural stiffness reduction factors for element ends A and B
γ = column to beam stiffness ratio = $(I_c/L_c)/(I_b/L_b)$
θ = rotation of deformed element chord
θ_A, θ_B = rotation at element ends A and B
θ_e = rotation from elastic analysis
θ_i = rotation from inelastic analysis
ρ' = axial force parameter used to calculated inelastic stability functions
σ_r = maximum residual stress
σ_y = yield stress
ζ = imperfection stiffness reduction factor
ψ_o = member out-of-plumbness imperfection